IJISET - International Journal of Innovative Science, Engineering & Technology, Vol. 10 Issue 04, April 2023
ISSN (Online) 2348 – 7968 | Impact Factor – 6.72
www.ijiset.com

Leveraging the Self-heating Effect of NTC Thermistor to Detect its Minimum Coverage by a Dispensed Paste in the Mass Production Process of Temperature Sensors.

Saúl Alejandro Rodríguez-Jiménez[1], Leonor Adriana Cárdenas-Robledo[2]

[1] Posgrado CIATEQ A.C., Cto. Aguascalientes Nte. 135, Parque industrial de Valle de Aguascalientes, Aguascalientes, Aguascalientes 20358, México.
[2] CIATEQ A.C., Centro de Tecnología Avanzada, Parque Industrial Tabasco Business Center, Cunduacán, Tabasco 86693, México.

Abstract

This paper develops a device capable of confirming the minimum coverage area on a thermistor by a thermal paste dispensed and cured in the manufacturing process of Exhaust Gas Recirculation (EGR) temperature sensors to provide the required fixation in the presence of mechanical shock conditions. Such a device leverages the thermistor's self-heating effect and the thermal conductivity of the paste to read the voltage drop from the sensor, which translates into paste coverage area. The methodology follows a synthesized procedure to develop equipment and processes, considering an early phase for concept confirmation to demonstrate the feasibility of the device development. In a later phase, the optimal parameters are calculated and set to the device for delivering the corresponding classification of the sensors during the test. Once launched in production, the device demonstrates high effectiveness in screening out the sensors with rejectable paste coverage area on the thermistor.

Keywords: *self-heating effect, thermistor, paste, temperature sensor, heat dissipation*

1. Introduction

The electrical-mechanical devices manufactured by modern industry increasingly incorporate data collection through sensors for decision-making [1], mainly in applications in which monitoring the current state of a system in terms of temperature is crucial, using sensors in direct contact with the system environment [2]. An example of this is used in vehicles with internal combustion engines and in their Exhaust Gas Recirculation (EGR) system [3], where temperature sensors are used to provide the electronic control unit [4] with information, which are also known as *EGR temperature sensors* [5]. The geometries of these EGR temperature sensors vary among different manufacturers. However, almost all of them have in common to have a thin and long metal probe that houses the sensitive element of the sensor [6]. They also have in common the use of a thermal paste or grease as a means of mechanical fixation and heat transfer between the probe and the thermistor [7], as observed in Figure 1.

The problem faced by a well-known company is that given the thixotropic nature [8] of the thermal paste they use (C575) and the difficulty of observing the inside of the probe once assembled the sensor, it is complex to ensure the amount and position in which it is deposited. Given this fact, it becomes uncertain that the C575 is in contact with the thermistor, covering it in a minimum area necessary to provide mechanical fixation in the presence of the shock and vibration test profile required by the customer [9].

There are currently a few devices employed to confirm the level of C575 paste coverage on the thermistor, including the use of a manually operated borescope [10] and with deep learning processing [11], the use of profilometer [12] and X-ray inspection [13]. However, these measuring instruments have some dependence in one way or another on humans, either to make a judgment or to operate them, not to mention the initial investment required in them.

To solve this problem, the company decided to develop an automatic device to confirm the coverage of the C575 paste on the thermistor and to ensure its mechanical fixation. This device takes advantage of the susceptibility of the thermistor to a physical effect known as *self-heating*, which occurs because the thermistor is basically a resistor that dissipates power in the form of heat when an electric current at a specific voltage flows through it [14].

Other electrical devices in which the self-heating effect is applied are water flow sensors [15], conventional air flow sensors [16] and seepage meters measuring slow groundwater inflows into water bodies, such as rivers and lakes [17].
Then, in combination with the thermal conductivity [18] of C575 paste and thermistor output voltage measurement [19], self-heating was leveraged for the development and implementation of a device to confirm paste coverage over thermistors in EGR temperature sensors; henceforth referred to as *Paste Coverage Test Device* (PCTD).

2. Materials and Methods

The PCTD development and implementation activities were carried out by following a synthesized procedure for the development of equipment and mass production processes shown in Figure 2, which comprises different phases from conceptualization to validation; each of the phases is discussed in the following sections.

2.1 Concept confirmation

As part of the company's manufacturing process of the EGR temperature sensors, the C575 paste is automatically dispensed right at the bottom of a metallic probe, in a confined "chamber" of difficult access and visibility using a stainless-steel needle of 7.6 cm in length. Later in the assembly process, a Negative Temperature Coefficient (NTC) thermistor [20] is inserted into this chamber. The cross-section image of Figure 1 shows the thermistor covered by the C575 paste that is in contact with the metal probe. Additionally, as result of the proposed concept test with EGR temperature sensors, it was possible to confirm that when the supply voltage between the thermistor terminals exceeds the manufacturer's recommendation, the self-heating effect is produced. Figure 3 shows an image from a thermographic camera in which a bare thermistor is self-heated after applying an overvoltage of 18 volts. The output voltage behavior of EGR temperature sensors with different C575 paste conditions when supplied with different voltages, appears in Figure 4.

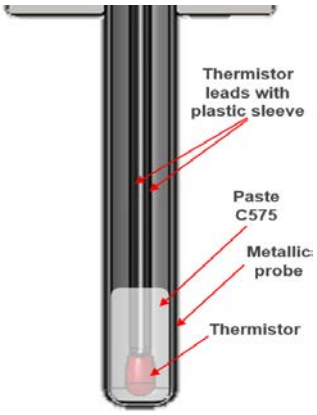

Figure 1. Temperature sensor.

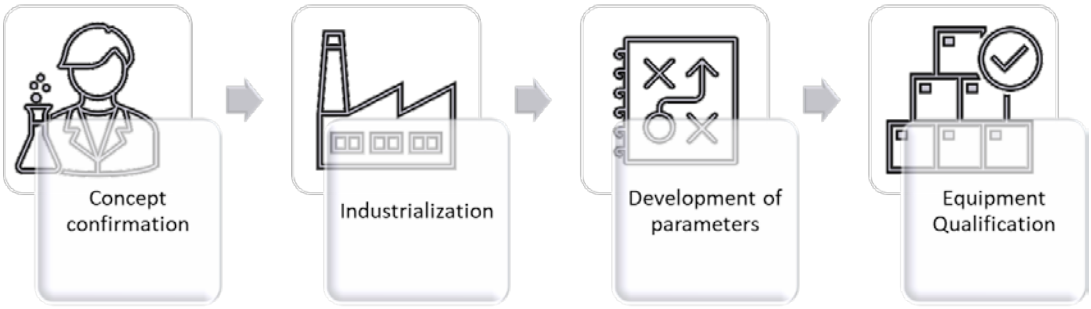

Figure 2. Synthesized procedure for the development of equipment and process.

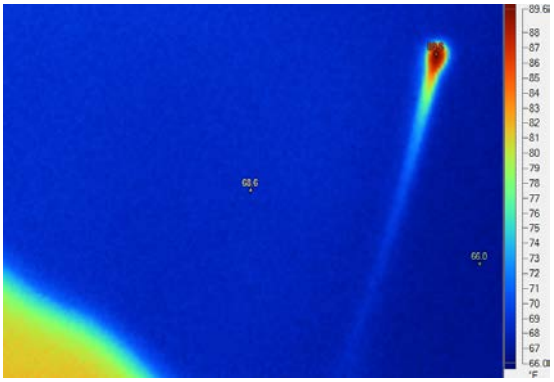

Figure 3. Thermistor self-heating after applying overvoltage.

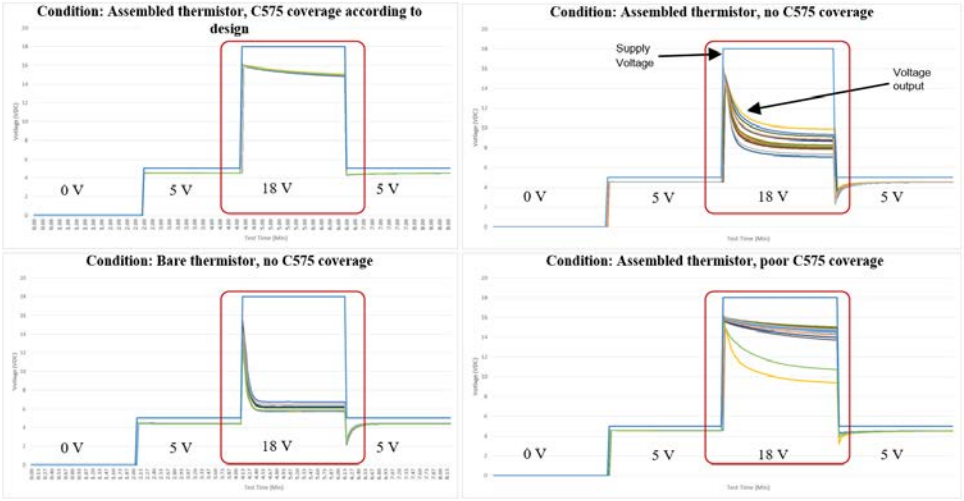

Figure 4. Behavior of voltage output measured in temperature sensors with different conditions of C575 coverage on thermistor

In the section enclosed in red corresponding to the 18 volts supply, it was possible to discern the most substantial difference in behavior between sensors with different C575 paste coverage conditions. For those sensors with coverage according to the product design (at least 2/3 thermistor), the rate of change in measured voltage with respect to time is less pronounced compared to those without coverage; this rate of change will refer to as *voltage drop across the thermistor* or simply *voltage drop* from now on. The less pronounced voltage drop in these sensors was attributed to the fact that the heat generated in the thermistor is conducted by the C575 paste (which is in contact with the self-heated thermistor) from the inside to the outside of the EGR temperature sensor (i.e., from the thermistor to the metal housing and then to the environment). Conversely, the more pronounced voltage drop in the parts without C575 paste coverage is explained by the buildup of heat generated in the thermistor due to its self-heating which has no means by which to be conducted to the outside. Table 1 summarizes this paragraph and incorporates the effect of thermistor self-heating on the electrical resistance of the thermistor.

The concept test incorporated the supply of 18 volts in EGR temperature sensors. However, the thermistor manufacturer warned that such voltage exceeded the maximum recommended power application (26 vs. 24 mW recommended) to avoid entering “runaway mode” and could potentially damage the thermistor. For this reason, the supply voltage of the PCTD is 11 volts. With this, the applied electrical power is reduced to 10 mW, which significantly reduced the risk of damage to the thermistor without compromising the self-heating necessary for the test at room temperature (25 °C). Figure 5 depicts the maximum possible amount of self-heating under such initial temperature conditions based on the Steinhart-Hart equation [21], which is 13.33°C. Considering these results, the potential to develop the PCTD for C575 paste coverage in the thermistor of EGR temperature sensors is confirmed.

2.2 Industrialization

This phase defines the indispensable elements for the suitability and acquisition of the hardware and software necessary to implement the PCTD, comprising different steps such as test algorithm, test parameters, parameter estimation tool, and production equipment design.

Test algorithm. The Final Function Test (FFT) production equipment was planned to incorporate the PCTD with the proper conditioning to introduce it and the ability to automatically store voltage readings observed during the sensor test time in an individual Excel file (one reading every 25 milliseconds). This provides information regarding heat generation and conduction in the sensor. Figure 6 plots three sets of these voltage readings, referred to as *voltage curves*.
The potential of the PCTD lies in the design of an algorithm that classifies the EGR temperature sensors according to their less or more pronounced voltage drop. It is achieved by taking voltage readings at different points of the curve (only two are required); the PCTD algorithm incorporates these readings in steps 5 and 6, as shown in Figure 7.

Table 1: Effect of thermistor self-heating effect in electrical resistance and voltage drop

Condition of paste C575 coverage on thermistor	Heat buildup in thermistor	Thermistor's electrical resistance	Voltage drop due to thermistor
According to design	Little	High	Low
No coverage	Much	Low	High

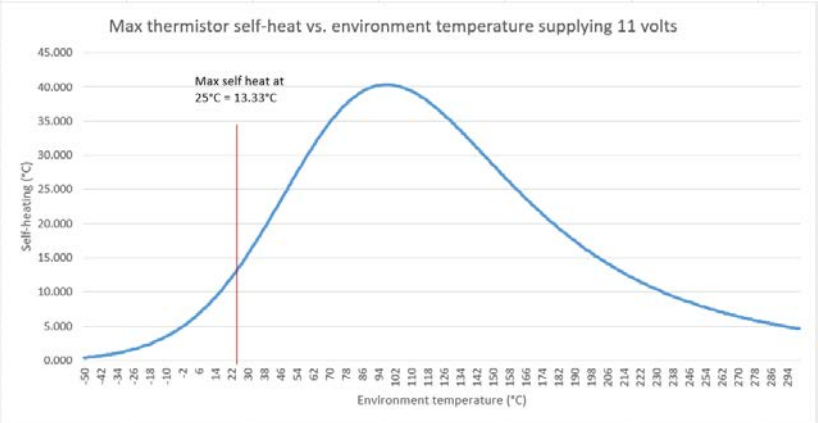

Figure 5. Curve of max self-heating in thermistor.

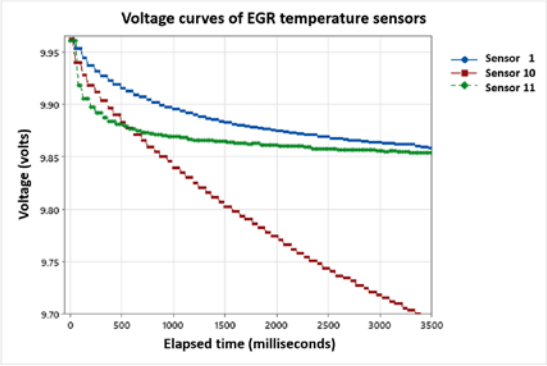

Figure 6. Voltage curves of different paste C575 coverage conditions

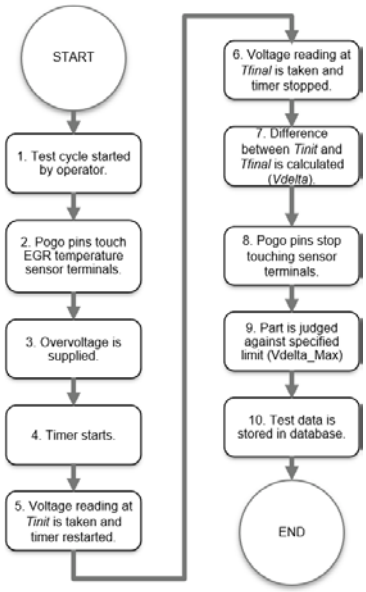

Figure 7. Algorithm to be implemented in the PCTD.

Test parameters. The developed parameters Tinit, Tfinal, and Vdelta_Max are implicit in the PCTD algorithm; in Figure 7 the step is referenced in parenthesis.

- *Tinit*. The instance of the timer measured in milliseconds at which the voltage reading 1 is taken (step 5).
- *Tfinal*. The instance of the timer measured in milliseconds at which the voltage reading 2 is taken (step 6).
- *Vdelta_Max*. The upper limit of voltage readings difference, hereafter referred to as *Vdelta* (step 9).

Parameter estimation tool. For the parameters *Tinit* and *Tfinal*, a tool was developed for their estimation from the voltage curves of each test. Such a tool was designed in *Excel* software to make use of the *Solver* module, which allows obtaining optimal solutions to complex problems by defining an optimization model [22]; from here on, the tool will be referred to as *Voltage Curve Analyzer* or simply as *Analyzer*.

The Analyzer uses a solution algorithm and the definition of numerical constraints to estimate Tinit and Tfinal values that produce the Vdelta values of known accepted EGR temperature sensors (with C575 paste coverage on thermistor according to design) consistently lower than those of known rejected sensors (without C575 paste coverage on thermistor). In other words, the goal is to maximize the difference between both types of sensors in the right direction: low Vdelta values for accepted sensors and high values for rejected sensors.

The Solver window with the parameters of the optimization model that the user must enter as part of the Analyzer (depicted in Figure 8) is briefly described next.

1. Objective function. It is selected in the window the direction of the optimization: minimizing, maximizing, or equaling a value. In the case of the Analyzer, the cell containing the indicator function of Eq. (1) was defined as the objective function, which represents the count of the times that the Vdelta value in the known rejected sensors are greater than the known accepted ones; it was selected in the Solver window that the objective function was maximized.

$$\sum_{\substack{1\le i\le m\\ 1\le j\le n}} \mathbb{1}_{(Vinit_i - Vfinal_i)<(Vinit_j - Vfinal_j)} \tag{1}$$

Where:

- o Vinit*i* and Vinit*j* represent the voltage readings at Tinit for the *i-th* known accepted sensor and the *j-th* known rejected sensor, respectively.
- o Vfinal*i* and Vfinal*j* represent the voltage readings at Tfinal for the *i-th* known accepted sensor and the *j-th* known rejected sensor, respectively.

2. Variables of the objective function. Although the parameters Tinit and Tfinal are not directly contained in the objective function, they do determine the calculation of the Vdelta value of the sensors, whether they are accepted or rejected. For this reason, these parameters were defined as the variables of the objective function, on which Solver iterated in search of the maximum value of the objective function.
3. Constraints. In any optimization problem, the values of the variables of the objective function need to be bounded in allowed ranges, which on many occasions have to do with the availability of resources or technological limitations. The elements that limit the variables are called *constraints*; Solver requests two types.
    a. Numeric. This constraint imposes limits to the value that the variable can take, either higher, lower, or integer. In the case of the Analyzer, individually and added together, the parameters Tinit and Tfinal must not be greater than 5000 milliseconds due to the cycle time of the FFT production equipment needing to be kept lower than this value. Also, both parameters are defined as integers (i.e., decimal values are not allowed).
    b. Non-negativity. This is the constraint used to represent the existence of resources, this is done by restricting the solution to involve negative numbers.
4. Solution algorithm. The solution method that Solver uses to find the optimal solution is selected. In the case of the Analyzer, the *evolutionary method* was defined, which is used to solve problems that do not have a linear solution.

Production equipment design. The last step in preparation for the implementation of the PCTD is to define in which of the stations of the FFT production equipment shown in Figure 9 the necessary changes needed to be incorporated. Table 2 lists the FFT equipment stations, their functions before and after the implementation of the PCTD; as can be seen from the table, the *Electrical continuity test* carried out at station 2 was consolidated at station 1 together with the *Electrical insulation test* in order to accommodate for the PCTD.

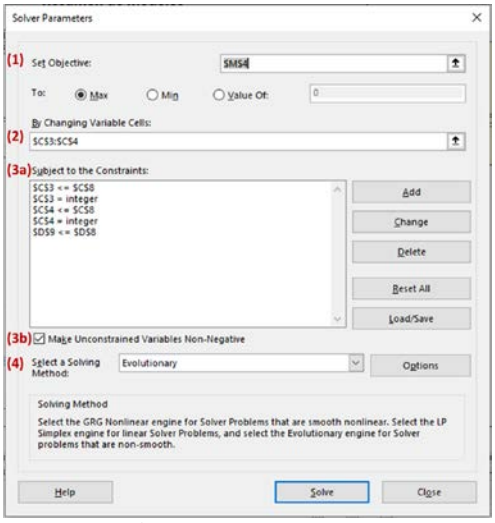

Figure 8. Configurable parameters in Solver module.

Table 2: Functions of stations in FFT production equipment before and after implementing PCTD

Station	Previous functions	Function after PCTD
St.0	Product load/unload	Product load/unload
St.1	Electrical insulation test	Electrical insulation and continuity test
St.2	Electrical continuity test	PCTD
St.3	Laser coding of good parts	Laser coding of good parts
St.4	Spare	Spare
St.5	Spare	Spare

2.3 Development of parameters.

As part of this section, activities necessary for the estimation of the parameters and sensor classification limit were carried out, once the PCTD was introduced in the FFT production equipment.

Estimation of Vinit and Vfinal. Twelve EGR temperature sensors were selected with varied coverage conditions, confirmed by X-Ray inspection, as depicted in Figure 10. The product design engineer specified clear criteria for acceptance and rejection of C575 paste coverage considering this inspection method, as shown in Table 3. These sensors were tested on the FFT production equipment: three replicates, each of the four positions (nests) of the machine tooling; all in random order. Figure 11 shows the order of the runs, which is the typical order followed when conducting a gage repeatability and reproducibility (GR&R) study [23]. Subsequently, the process data that the FFT production machine automatically saved to the server was downloaded and verified that there was no problem with data storage.

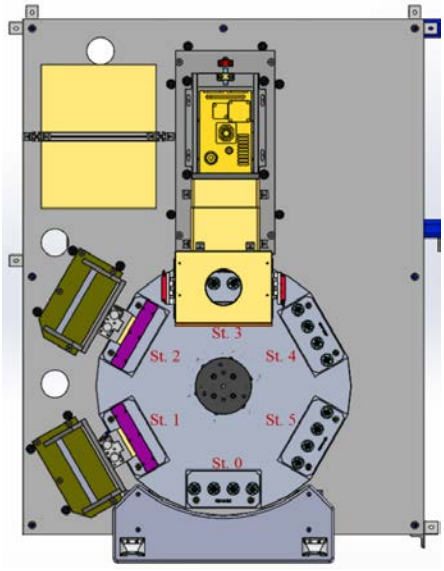

Figure 9. Stations of FFT production equipment.

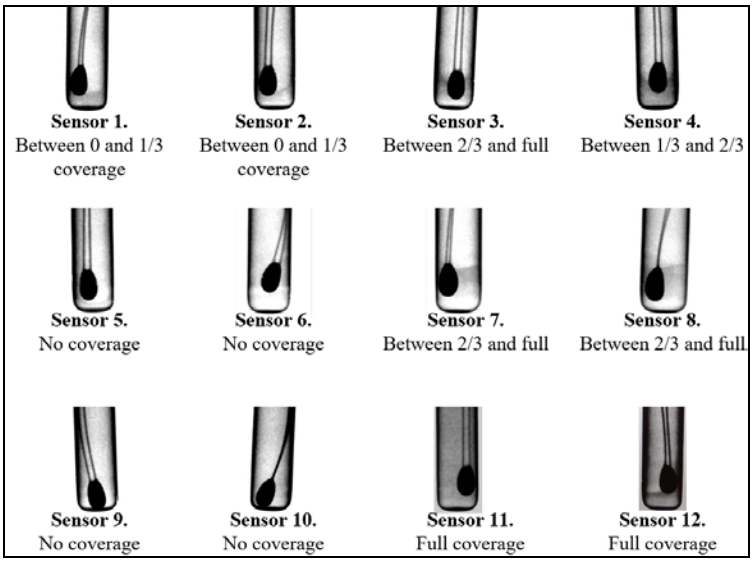

Figure 10. Coverage condition of C575 paste in EGR temperature sensors used in GR&R study.

In addition to downloading the process data that was stored on the server, the voltage curves were also obtained and entered in the Analyzer (a total of 144 curves). Then, the algorithm was run in Solver, which found an optimal solution in approximately 40 seconds, estimating the Tinit and Tfinal parameter values in 1370 and 1480 milliseconds. These estimated values effectively produced maximization of the objective function. In other words, in each of the opportunities (2211 in total) for comparison of Vdelta values between the accepted and rejected sensors, the latter were always greater than the former, and in none of the comparisons did this happen the other way around. In addition to this, the means for the three groups of sensors that are summarized according to their status label in the *Table of statistics* in Figure 12 were observed to be substantially different. This was confirmed by the two-sample T-test, which produced a *P-value* lower than 0.05, typically used. Also, a clear separation between the three boxes representing the results of the three types of sensors according to their status label was observed in the boxplot of Figure 13 which supports statement above.

Table 3: Acceptance and rejection criteria of C575 paste coverage in thermistors.

Condition of paste C575 coverage on thermistor	**Criteria**	**Reaction plan**	**Label in Analizer tool**	**Example of sensors in Figure 10.**
No coverage	Reject	Dispose in scrap bin	R_null	5, 6
Between 0 and 1/3	Reject	Segregate for Analysis	R_partial	1, 2
Between 1/3 and 2/3	Reject	Segregate for Analysis	R_partial	4
Between 2/3 and full	Accept	Keep processing	A_par_tot	3, 7
Full coverage	Accept	Keep processing	A_par_tot	11, 12

	Nest	Replicate 1				Replicate 2				Replicate 3			
		1	**2**	**3**	**4**	**1**	**2**	**3**	**4**	**1**	**2**	**3**	**4**
Run	**1**	1	2	3	4	12	11	10	9	2	5	11	4
	2	5	6	7	8	8	7	6	5	1	7	3	10
	3	9	10	11	12	4	3	2	1	9	6	8	12
	4	4	1	2	3	9	12	11	10	4	2	5	11
	5	8	5	6	7	5	8	7	6	10	1	7	3
	6	12	9	10	11	1	4	3	2	12	9	6	8
	7	3	4	1	2	10	9	12	11	11	4	2	5
	8	7	8	5	6	6	5	8	7	3	10	1	7
	9	11	12	9	10	2	1	4	3	8	12	9	6
	10	2	3	4	1	11	10	9	12	5	11	4	2
	11	6	7	8	5	7	6	5	8	7	3	10	1
	12	10	11	12	9	3	2	1	4	6	8	12	9

Figure 11. Run order of EGR temperature sensors in GR&R study.

Results summary

Table of statistics

	R_null	R_partial	A_par_tot
n	48	48	48
Mean	0.0729	0.0229	0.0121
Std. Dev	0.02644	0.00448	0.00217

t-Test 6.4471E-19 Difference between A y R

Table of counts

Condition	Count
R - A >0	0
R - A <=0	0
Sum of square	0

Figure 12. Summary of results optimized by Solver.

Estimation of Vdelta_Max. Once Vinit and Vfinal parameters were estimated, the next step was to estimate the Vdelta_Max parameter based on the calculated Vdelta values. For this, the PCTD process data was collected from 3 production batches, equivalent to 3 thousand sensors. These sensors were inspected with X-rays in order to correlate the numerical value with an image. Once tested in the PCTD, the data was analyzed using the frequency histogram shown in Figure 14, which showed that the data did not seem to be normally distributed. Actually, the distribution of the Vdelta values tended to form three almost perfectly defined groups: the first one from left to right resembled a Normal distribution having as border values 0 to 0.015; the second had a more flattened shape going from 0.015 to 0.047; finally the third one appeared to have a slightly more pointed shape, starting from 0.047 to just over 0.1. For group 1, normality of the data was demonstrated in Figure 15.

Then, using the PCTD process data and the X-Ray inspection images from each sensor, a random sample from each of the groups was taken to identify what level of C575 paste coverage they had. A correspondence of Vdelta values of group 1 and the pieces with acceptance criteria was found; same finding with values of group 2 and the pieces with partial coverage and "segregate for analysis" criteria; and with values of group 3 and null coverage; these criteria are shown in Table 3.

X-ray images of EGR temperature sensors with Vdelta values coming from each of the three groups are shown in Figure 16.

Based on the X-ray images of the three groups (especially those of groups 1 and 2), the value of the Vdelta_Max parameter was estimated in 0.015, under which the EGR temperature sensors were judged during the *Launch control* period.

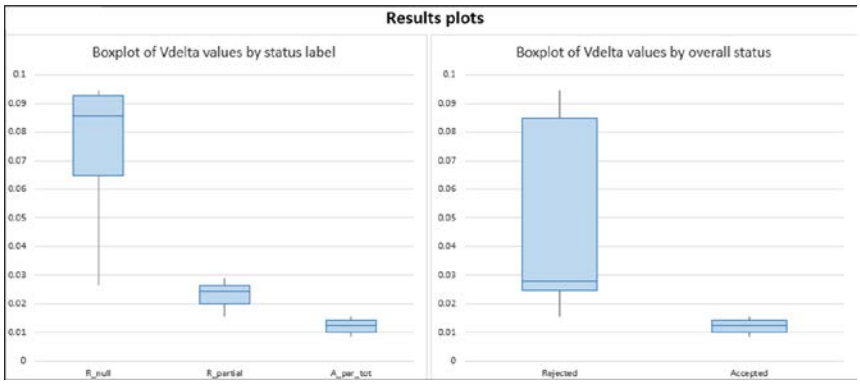

Figure 13. Plots of results optmized by Solver.

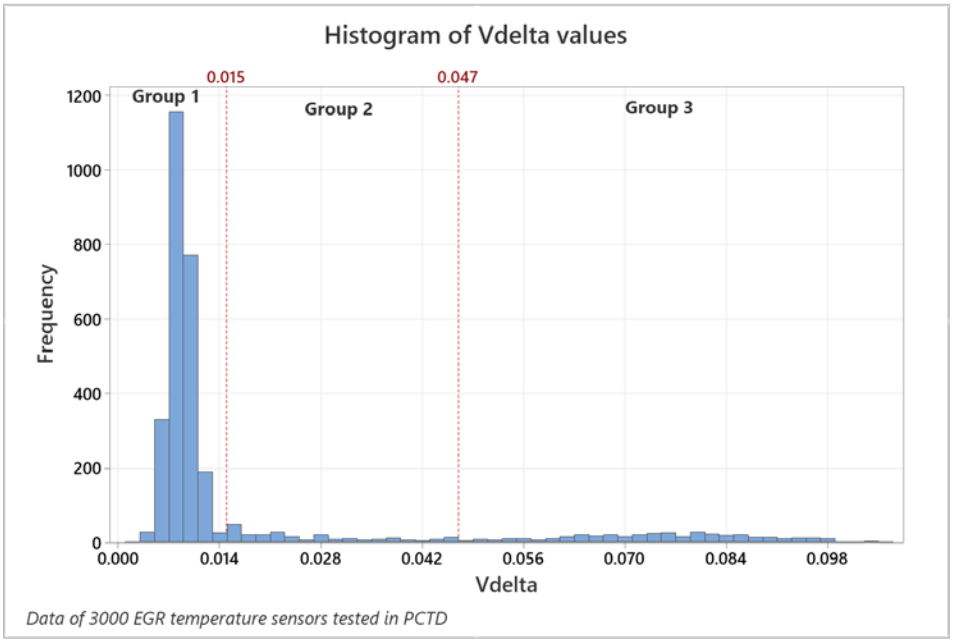

Figure 14. Histogram of Vdelta values from 3000 EGR temperature sensors.

IJISET - International Journal of Innovative Science, Engineering & Technology, Vol. 10 Issue 04, April 2023
ISSN (Online) 2348 – 7968 | Impact Factor – 6.72
www.ijiset.com

2.4 Validation plan.

The validation plan for the implementation of the PCTD in the FFT production equipment consisted of a GR&R study and a process capability study (Cpk) [24], both are shown in Figure 17 and Figure 18, respectively.
In Figure 17, in the *Gage Evaluation* section, the *%Study Var* (or Percentage of variation) of the source called *Total Gage R&R* (or Total Gage Repeatability and Reproducibility of the study) is shown which was less than 10%, this is the maximum value that a GR&R study can obtain for the measurement system to be considered as acceptable. This study was carried out with 12 EGR temperature sensors tested in the run order shown in Figure 11.
Also, Figure 18 shows the Cpk study of the first production batch, in which the *Cpk* value was greater than 1.33 which is the lower limit for a process to be considered capable of producing parts within the technical specification [25].
Based on these studies, the implementation of the PCTD was considered validated and ready to test in mass production.

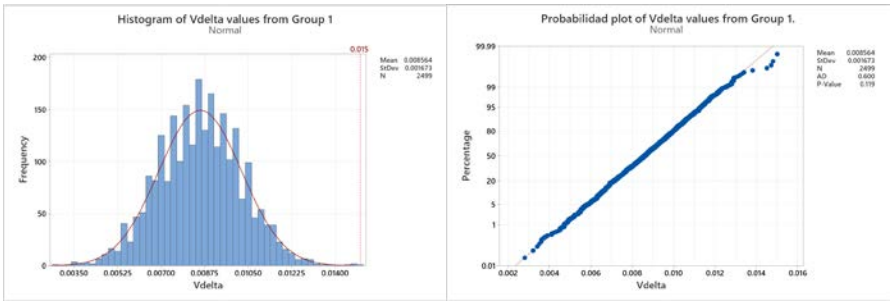

Figure 15. Histogram and probability plot of Vdelta values from Group 1.

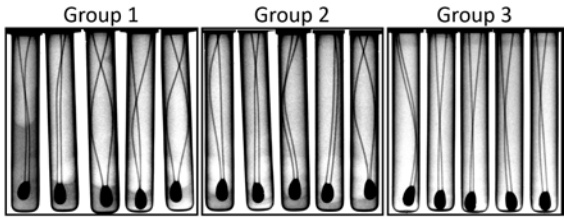

Figure 16. X-ray images sampled from all groups.

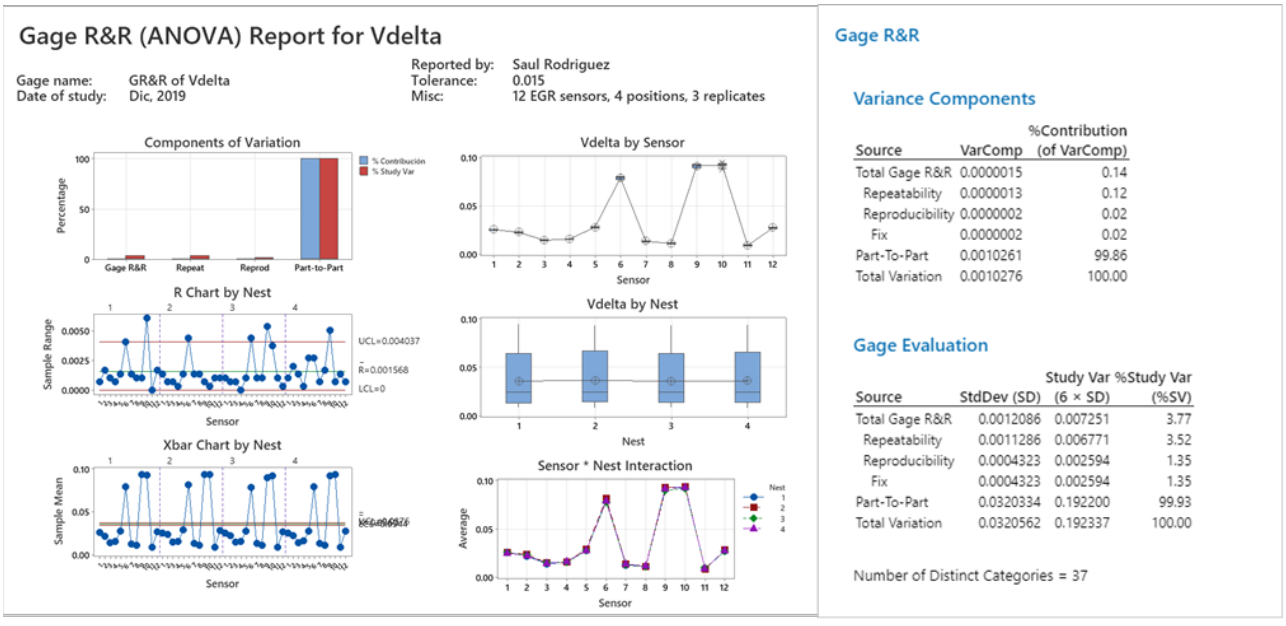

Figure 17. GR&R study of Vdelta values.

3. Results and discussion

In the Launch control period, EGR temperature sensors were produced and tested with the PCTD active in 10 production lots (each with 1050 EGR temperature sensors). Then they were inspected by X-Ray, and the number of sensors accepted and rejected by the PCTD appears in Table 4. Subsequently, both categories of sensors were X-ray inspected (treated separately) and classified into one of the C575 paste coverage condition categories listed in Table 3; this information was summarized and reported in Tables 5 and 6 for the rejected and accepted sensors, respectively.

From Table 5, which includes the breakdown of the C575 paste coverage conditions in the sensors rejected by the PCTD, in a high percentage of them (66.6%), the rejection was correct; the condition included is *No coverage*. Also, according to the acceptance criteria in Table 3, 28.98% of the rejected sensors belonged to the "Segregate for analysis" group; the conditions included are coverage *Between 0 and 1/3* thermistor and coverage *Between 1/3 and 2/3* thermistor. And finally, 4.34% of the sensors were incorrectly rejected (type 1 error) or over-segregated; the conditions included are coverage *Between 2/3 and full* thermistor and *Full coverage*.

Regarding Table 6, which breaks down the C575 paste coverage conditions in the sensors accepted by the PCTD, 0.42% of the sensors exhibited a condition that implied segregation for analysis, and the PCTD did not detect it. It indicates that the conditions included in these sensors are probably not rejectable. However, an exhaustive analysis must be carried out, and later approval must be provided by the product design engineer for these conditions to be accepted. Also, none of the accepted sensors were found with *No coverage* condition of C575 paste.

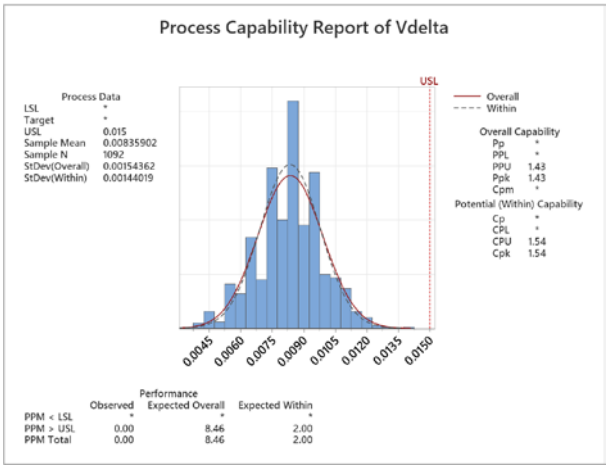

Figure 18. Cpk study of Vdelta values.

Table 4: Overall summary of accepted and rejected sensors by the PCTD.

Lot number	Accepted by PCTD	Rejected by PCTD
J01, 44326756	1046	4
J02, 44326757	1031	19
J03, 44320933	1050	0
J04, 44319599	1025	25
J05, 44319605	1043	7
J06, 44314439	1041	9
J07, 44330540	1048	2
J08, 44330541	1049	1
J09, 44334931	1048	2
J10, 44334934	1050	0

Table 5: X-ray inspection results of rejected sensors by the PCTD, classified by C575 paste coverage condition.

Lot number	No coverage	Between 0 and 1/3	Between 1/3 and 2/3	Between 2/3 and full	Full coverage
J01, 44326756	3	1	0	0	0
J02, 44326757	15	1	0	1	2
J03, 44320933	0	0	0	0	0
J04, 44319599	13	11	1	0	0
J05, 44319605	7	0	0	0	0
J06, 44314439	5	2	2	0	0
J07, 44330540	2	0	0	0	0
J08, 44330541	1	0	0	0	0
J09, 44334931	0	2	0	0	0
J10, 44334934	0	0	0	0	0

Table 6: X-ray inspection results of accepted sensors by the PCTD, classified by C575 paste coverage condition.

Lot number	No coverage	Between 0 and 1/3	Between 1/3 and 2/3	Between 2/3 and full	Full coverage
J01, 44326756	0	0	1	0	1045
J02, 44326757	0	0	0	0	1031
J03, 44320933	0	0	0	0	1050
J04, 44319599	0	4	11	6	1004
J05, 44319605	0	0	1	2	1040
J06, 44314439	0	17	8	2	1014
J07, 44330540	0	0	0	6	1042
J08, 44330541	0	0	0	0	1049
J09, 44334931	0	0	2	2	1044
J10, 44334934	0	0	0	0	1050

4. Conclusions

This paper presented the problem faced by a company in the manufacturing process of EGR sensors related to paste coverage detection in such sensors. The approach proposed comprised the development and implementation of the PCTD, an automatic device that confirms the coverage area of the C575 paste on the thermistor to ensure its mechanical fixation. The PCTD takes advantage of the susceptibility of the thermistor to self-heating and the thermal conductivity of the C575 paste. Moreover, the PCTD was successfully implemented in the company's mass production process of EGR temperature sensors. During the Launch control trial, none was found with the *No coverage* condition, indicating a high effectiveness of the PCTD to detect the sensors with rejectable conditions.

References

[1] Kumar S., Tiwari P., and Zymbler M., "Internet of Things is a Revolutionary Approach for Future Technology Enhancement: A Review ", Journal of Big Data, Vol. 6, No. 111, 2019, pp. 001-021.
[2] Semakula M. and Inambao F., "The Effects of Exhaust Gas Recirculation on the Performance and Emission Characteristics of a Diesel Engine – A Critical Review ", International Journal of Applied Engineering Research ISSN 0973-4562, Vol. 12, No. 23, 2017, pp. 13677-13689.
[3] Zhao W. Z, Sun T., Grattan Keneth T V, Lucas J., and Al-Shamma'a A. I., "Temperature Monitoring of Vehicle Engine Exhaust Gases Using Optical Fibre Temperature Sensor Systems", in 17th International Conference on Optical Fibre Sensors, Vol. 5855, 2005, pp. 832-835.
[4] Tutunea D., Ilie D., Racila L., Otat O., and Geonea I., "Evaluation of Temperature Sensors Used in Automotive Applications Type NTC and PTC", IOP Conference: Materials Science and Engineering, Vol. 1220, No. 012035, 2022, pp. 001-006.
[5] Rakopoulos C. D., Rakopoulos D. C., Mavropoulos G. C., and Kosmadakis G. M., "Investigating the EGR rate and temperature impact on diesel engine combustion and emissions under various injection timings and loads by comprehensive two-zone modeling", Energy, Vol. 157, No. 1, 2018, pp. 990-1014.
[6] Ahmed I., "Engine Coolant Temperature Sensor in Automotive Applications", Technical Report Submitted in Fulfilment of the Requirements for the Academic Degree, Department of Automotive Software Engineering, Technische Universitat Chemnitz, Chemnitz, Germany, 2020.
[7] He Y., "Rapid Thermal Conductivity Measurement with a Hot Disk Sensor: Part 2. Characterization of Thermal Greases", Thermochimica Acta, Vol. 436, No. 1-2, 2005, pp. 130-134.
[8] Larson G., "Constitutive Equations for Thixotropic Fluids", Journal of Rheology, Vol. 59, No. 3, 2015, pp. 595-611
[9] Hanly S. W., "Shock & Vibration Testing Overview", Woburn: Midé Technology Corporation, 2016.
[10] Zhongda Y., and Mingguang L., "Specification for Engine Borescope Inspection Report", IOP Conf. Ser.: Earth Environ. Sci., Vol. 186, No. 5, 2018, pp. 001-005.
[11] Shang H., Sun C., Liu J., Chen X., and Yan R., "Deep Learning-Based Borescope Image Processing for Aero-Engine Blade In-Situ Damage Detection", Aerospace Science and Technology, Vol. 123, No. 107473, 2022, pp. 001-014.
[12] Mital G., Dobránsky J., Ružbarský J., and Olejárová Š., "Application of Laser Profilometry to Evaluation of the Surface of the Workpiece Machined by Abrasive Waterjet Technology", Appl. Sci., Vol. 9, No. 10, 2019, pp. 001-014.
[13] Shashishekhar N., "Automated X-Ray Inspection: Industrial Applications and Case Studies", e-Journal of Nondestructive Testing, Vol. 22, No. 6, 2017, pp. 139-144.
[14] Ebrahimi-Darkhaneh H., "Measurement Error Caused by Self-Heating in NTC and PTC Thermistors", Analog Design Journal, Vol 3Q, No. 4, 2019, pp. 001-007.
[15] Nikolic M. V., Radojcic B. M., Aleksic O. S., and Lukovic M., "A Thermal Sensor for Water Using Self-Heated NTC Thick-Film Segmented Thermistors", IEEE Sensors Journal, Vol. 11, No. 8, 2011, pp. 1640-1645.
[16] Xu C., Guo X., Jiang H., Zhang Z., and Liu S., "Modeling and Simulation of Self-Heating Effect with Temperature Difference Air Flow Sensor", in 15th International Conference on Electronic Packaging Technology, Vol. 2014, 2014, pp. 655-659.
[17] Skinner A. J., and Lambert M. F., "Evaluation of a Warm-Thermistor Flow Sensor for Use in Automatic Seepage Meters", IEEE Sensors Journal, Vol. 9, No. 9, 2009, pp. 1058-1067.
[18] Yang Y., Physical Properties of Polymers Handbook, Cincinnati: Springer, 2007.
[19] Kima J., and Kim J. D., "Voltage Divider Resistance for High-Resolution of the Thermistor Temperature Measurement", Journal of the International Measurement Confederation, Vol. 44, No. 10, 2011, pp. 2054-2059.
[20] Iyere S., Ozigi B., and Yeboah J., "Response Characteristics of a Negative Temperature Coefficient Thermistor", Journal of Electrical, Control and Telecommunication Research, Vol. 1, No. 113, 2020, pp. 017-022.
[21] Petkovšek M., Nemec M., and Zajec P., "Algorithm Execution Time and Accuracy of NTC Thermistor-Based Temperature Measurements in Time-Critical Applications", Mathematics, Vol. 9, No. 2066, 2021, pp. 001-016.
[22] Kota L., and Jarmai K., "Efficient Algorithms for Optimization of Objects and Systems", An International Journal for Engineering and Information Sciences, Vol. 9, No. 1, 2014, pp. 121-132.
[23] Munro R., Ramu G., and Zrymiak D., The Certified Six Sigma Green Belt Handbook, Milwaukee: ASQ, 2015.
[24] Arcidiacono G., and Nuzzi S., "A Review of the Fundamentals on Process Capability, Process Performance, and Process Sigma, and an Introduction to Process Sigma Split", International Journal of Applied Engineering Research, Vol. 12, No. 14, 2017, pp. 4556-4570.
[25] Gutierrez H., and de la Vara R., Control Estadístico de la Calidad y Seis Sigma, Mexico DF: McGraw Hill, 2013.

First Author Saúl Alejandro Rodríguez-Jiménez received the B.Sc. degree in Industrial Engineering from the Aguascalientes Technological Institute in 2015 and a specialization in Statistical methods by Center for Research in Mathematics in 2018, he is now a master's student in Advanced Manufacturing at CIATEQ, Aguascalientes, Mexico.

Second Author Leonor Adriana Cárdenas-Robledo is a researcher at Centro de Tecnología Avanzada (CIATEQ), Mexico. She holds an M. Sc. in Computer Science and a Ph.D. in Systems Engineering. Her research focuses on ubiquitous learning, virtual and augmented reality, and technology-enhanced learning. She is a National Researcher of Mexico (CONACYT-SNI), Level I.